Horsten, N.; Groth, M.; Blommaert, M.; Dekeyser, W.; Pérez, I. Paradela; Wiesen, S.; JET Contributors

Application of spatially hybrid fluid–kinetic neutral model on JET L-mode plasmas

Published in:
Nuclear Materials and Energy

DOI:
10.1016/j.nme.2021.100969

Published: 01/06/2021

Document Version
Publisher's PDF, also known as Version of record

Nuclear Materials and Energy 27 (2021) 100969

Contents lists available at ScienceDirect

Nuclear Materials and Energy

journal homepage: www.elsevier.com/locate/nme

Application of spatially hybrid fluid–kinetic neutral model on JET L-mode plasmas

N. Horsten [a,b,*], M. Groth [a], M. Blommaert [c], W. Dekeyser [c], I. Paradela Pérez [a,d], S. Wiesen [e], JET Contributors[1]

[a] Aalto University, Department of Applied Physics, FI-00076, AALTO, Finland
[b] EUROfusion Consortium, JET, Culham Science Centre, Abingdon, OX14 3DB, United Kingdom
[c] KU Leuven, Department of Mechanical Engineering, Celestijnenlaan 300A, 3001 Leuven, Belgium
[d] Max-Planck-Institut für Plasmaphysik, Garching, Germany
[e] Forschungszentrum Jülich, Institut für Energie- und Klimaforschung - Plasmaphysik, D-52425 Jülich, Germany

ARTICLE INFO

Keywords:
Plasma edge modeling
Neutrals
Kinetic model
Fluid approximation

ABSTRACT

We present a spatially hybrid fluid–kinetic neutral model that consists of a fluid model for the hydrogen atoms in the plasma grid region coupled to a kinetic model for atoms sampled at the plasma–void interfaces and a fully kinetic model for the hydrogen molecules. The atoms resulting from molecular dissociation are either treated kinetically (approach 1) or are incorporated in the fluid model (approach 2). For a low-density JET L-mode case, the hybrid method reduces the maximum fluid–kinetic discrepancies for the divertor strike-point electron densities and electron temperatures from approximately 150% to approximately 20% for approach 1 and to approximately 40% for approach 2. Although the simulations with purely fluid neutral model become more accurate for increasing upstream plasma density, we still observe a significant improvement by using the hybrid approach. When consuming the same CPU time in averaging the electron strike-point densities and temperatures over multiple iterations as for the simulations with fully kinetic neutrals, hybrid approach 1 reduces the statistical error with on average a factor 2.5. Hybrid approach 2 further increases this factor to approximately 3.3, at the expense of accuracy.

1. Introduction

To simulate the particle and energy transport in edge plasmas, a fluid model for the ions and electrons is typically coupled to a kinetic model for the neutral atoms and molecules. SOLPS-ITER is an example of a plasma edge code suite [1,2]. It consists of the B2.5 code for a finite-volume solution of the plasma fluid equations coupled to the EIRENE code for a Monte Carlo (MC) simulation of the kinetic equation for the neutral particles [3].

A kinetic treatment for the neutrals facilitates the incorporation of multiple atomic and molecular processes as well as the treatment of complex geometries. However, the kinetic MC method comes at a large computational cost for highly-collisional detached cases. A simulation of ITER in the (partially) detached regime can, for example, take several months [4]. For this reason, there is an increased interest in the use of (partially) fluid models for the neutrals. The increased collisionality of atoms in the detached regime justifies a fluid description in some parts of the plasma edge. Therefore, approximate fluid neutral models are in use since decades, see, e.g., Refs. [5–7].

Besides the fact that a fluid closure can introduce significant errors, there are two additional shortcomings with the use of a purely fluid model for the neutrals. Firstly, the fluid neutral approximation is typically exclusively used in the plasma grid region (green area in Fig. 1). This implies that the neutral transport in the void regions is neglected and artificial boundary conditions have to be imposed at the last simulated flux surfaces in the private-flux (PF) and scrape-off-layer (SOL) regions. Secondly, whereas the mean free path of the hydrogen atoms is indeed reduced for detached scenarios due to an increased number of charge-exchange collisions, it is far from clear if the fluid limit is also reached for the hydrogen molecules and impurity species.

In this paper, we aim to eliminate these additional shortcomings by using a spatially hybrid fluid–kinetic model for the hydrogen atoms coupled to a fully kinetic model for the molecules. Kinetic atoms are sampled at the plasma–void interfaces and traced across the void regions to incorporate the neutral transport in the vacuum zones. The spatially hybrid approach for plasma edge neutrals is introduced in

* Corresponding author at: Aalto University, Department of Applied Physics, FI-00076, AALTO, Finland.
E-mail address: niels.horsten@aalto.fi (N. Horsten).
[1] See the author list of E. Joffrin et al., Nuclear Fusion 59 (2019) 112021.

https://doi.org/10.1016/j.nme.2021.100969
Received 31 July 2020; Received in revised form 1 March 2021; Accepted 9 March 2021
Available online 15 March 2021

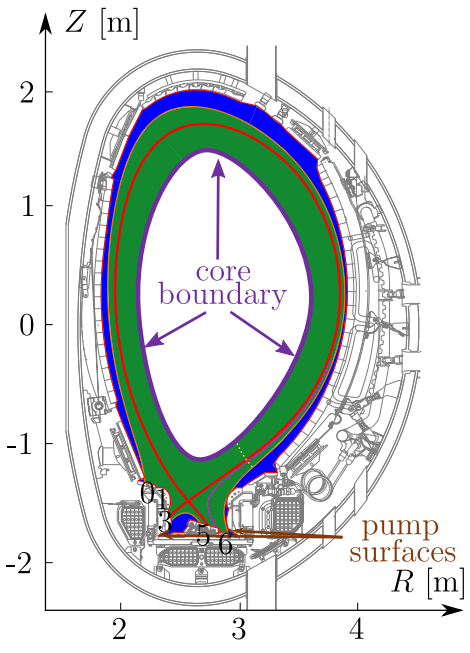

Fig. 1. Poloidal cross-section of JET tokamak: the green and blue areas respectively correspond to the plasma fluid domain and the void regions. The poloidal flux tube indicated with the pink dashed line (at approximately 5 cm outer target surface length in the SOL) and the radial location indicated with the yellow dotted line (with a poloidal distance along the separatrix of approximately 1 m from the outer target) are used to assess the neutral density profiles in Section 4.2. The relevant target tile numbers are indicated. In our plasma grid, the step between tiles 5 and 6 is less steep.

Ref. [8]. However, in that paper it is only applied to a simplified rectangular slab case in the absence of molecules. In this contribution, we couple the spatially hybrid atom model to a fully kinetic molecule model and we assess the results for a realistic JET case. The application of the hybrid δf method from Ref. [9], to eliminate the fluid closure errors within the plasma domain itself, is kept as future research.

2. Model description

The spatially hybrid model is implemented in SOLPS-ITER, in which the B2.5 part solves the Braginskii equations parallel to the magnetic field for the electron and ion species [10], superposed with a simple diffusion model for the turbulent transport perpendicular to the magnetic field. Although SOLPS-ITER contains the different electromagnetic drift contributions [11], including the drift terms is out of the scope of this paper. The plasma model consists of a continuity and parallel momentum equation for each individual plasma species, an electron energy equation, and an (internal) ion energy equation. All electric currents are set to zero and the potential is set to $3.1T_e/q$, with T_e the electron temperature and q the elementary charge.

2.1. Fluid neutral model

In the plasma fluid domain (green area in Fig. 1), we solve a fluid model for the hydrogen atoms that consists of a continuity and parallel momentum equation, solved for the atom density n_a and parallel velocity $u_{a\|}$. The atom transport perpendicular to the magnetic field is assumed to be governed by the pressure gradient. We assume that the fluid atoms have the same temperature as the main ions (T_i) and the fluid atom energy transport terms and sources are added to the ion energy equation. More detailed expressions for the fluid neutral model equations, as implemented in B2.5, can be found in Ref. [12].

At the plasma grid boundaries, we impose fluid neutral particle, parallel momentum, and energy fluxes as boundary conditions for the fluid neutral equations. We assume that the core boundary is far enough inside the separatrix to set the fluid neutral fluxes to the core to zero. At the divertor targets and plasma–void interfaces, we obtain the boundary fluxes by taking the particular moments of the assumed underlying atom particle-velocity distribution. At each boundary (except at the core boundary), we assume that the velocity distribution of the incident atoms is a truncated Maxwellian. The velocity-dependent particle flux vector $\mathbf{\Gamma}_a(\mathbf{v})$ at a boundary can be written as

$$\mathbf{\Gamma}_a(\mathbf{v}) = n_a \left(\frac{m}{2\pi T_i}\right)^{3/2} \exp\left(-\frac{m}{2T_i}\|\mathbf{v} - u_{a\|}\mathbf{e}_\|\|^2\right)\mathbf{v}, \quad \text{for } \mathbf{v}\cdot\boldsymbol{\nu} \le 0, \tag{1}$$

with $\mathbf{v}$ the particle-velocity vector, m the particle mass, $\mathbf{e}_\|$ the unit vector parallel to the magnetic field, and $\boldsymbol{\nu}$ the boundary normal pointing into the plasma region. It should be noted that all state variables and the surface normal vector depend on the spatial position, but this dependence is omitted in the notation. We assume in Eq. (1) that the fluid atom velocity only has a component parallel to the magnetic field.

The velocity distribution of the recycled/reflected atoms is obtained by integrating the incident ion distribution ($\mathbf{\Gamma}_i(\mathbf{v})$) and fluid atom distribution multiplied by the reflection kernel over the incident velocity space ($\int_{\mathbf{v}'\cdot\boldsymbol{\nu}\le 0} \ldots \mathrm{d}\mathbf{v}'$):

$$\mathbf{\Gamma}_a(\mathbf{v}) = -\int_{\mathbf{v}'\cdot\boldsymbol{\nu}\le 0} R_f(\mathbf{v}')R(\mathbf{v}'\to\mathbf{v})(\mathbf{\Gamma}_i(\mathbf{v}') + \mathbf{\Gamma}_a(\mathbf{v}'))\mathrm{d}\mathbf{v}', \quad \text{for } \mathbf{v}\cdot\boldsymbol{\nu} > 0, \tag{2}$$

where $R_f(\mathbf{v}')$ is the probability that the incident ion or atom with velocity $\mathbf{v}'$ is reflected as an atom and $R(\mathbf{v}'\to\mathbf{v})$ gives the velocity distribution of the reflected particle. The reflection kernel properties depend on the surface material. In this paper, we use the TRIM database [13] for the reflection properties. Because the recycling sources at the plasma–void interfaces are treated kinetically and the incident fluid atoms are assumed to be emitted as kinetic atoms into the void region (see Section 2.2), $R_f(\mathbf{v}') \equiv 0$ at the plasma–void interfaces. The ion distribution is assumed to be a truncated Maxwellian accelerated by the sheath potential, i.e.,

$$\mathbf{\Gamma}_i(\mathbf{v}) = \begin{cases} C_i\left(\frac{m}{2\pi T_i}\right)^{3/2} \exp\left(-\frac{m}{2T_i}\left\|\mathbf{v} - \mathbf{V}_i - \sqrt{\frac{2\delta_{sh}^{pot}T_e}{m}}\boldsymbol{\nu}\right\|^2\right)\mathbf{v}, & \text{if } \mathbf{v}\cdot\boldsymbol{\nu} \le -\sqrt{\frac{2\delta_{sh}^{pot}T_e}{m}}, \\ 0, & \text{otherwise,} \end{cases} \tag{3}$$

with $\mathbf{V}_i$ the ion fluid velocity vector at the sheath entrance and δ_{sh}^{pot} the sheath coefficient. The scaling factor C_i guarantees that the zeroth order moment corresponds to the macroscopic particle flux, i.e., $-\int_{\mathbf{v}\cdot\boldsymbol{\nu}\le 0} \mathbf{\Gamma}_i(\mathbf{v})\cdot\boldsymbol{\nu}\mathrm{d}\mathbf{v} = \Gamma_i$, with Γ_i the incident ion particle flux density.

Combining Eqs. (1)–(2) for the incident ($\mathbf{v}\cdot\boldsymbol{\nu} \le 0$) and reflected ($\mathbf{v}\cdot\boldsymbol{\nu} > 0$) velocity distributions, respectively, leads to the total estimated atom velocity distribution at a boundary point. The particle flux density Γ_a, parallel momentum flux density $\Gamma_{m\|,a}$, and energy flux density Q_a follow from the particular moments:

$$\begin{bmatrix}\Gamma_a & \Gamma_{m\|,a} & Q_a\end{bmatrix}^T = \int_{\mathbf{v}} \begin{bmatrix}1 & m\mathbf{v}\cdot\mathbf{e}_\| & m\|\mathbf{v}\|^2/2\end{bmatrix}^T \mathbf{\Gamma}_a(\mathbf{v})\cdot\boldsymbol{\nu}\mathrm{d}\mathbf{v}, \tag{4}$$

with $\int_{\mathbf{v}} \ldots \mathrm{d}\mathbf{v}$ the integral over the whole velocity space. More details on the implementation of this kind of boundary conditions can be found in Ref. [14].

We use the 9-point stencil discretization for all equations. This becomes in particular essential to account for the isotropic character of the neutrals, when using a fluid neutral model [15].

2.2. Kinetic neutral model

The fluid plasma and hydrogen atom models are coupled to EIRENE for the simulation of the MC trajectories of the kinetic atoms and molecules. Although the hybrid model for hydrogen isotopes could be

easily coupled to a kinetic model for the neutral impurity species, we consider a pure deuterium plasma only in this paper.

There are three types of kinetic source strata: (i) atoms and molecules resulting from ion recycling at the plasma–void interfaces; (ii) atoms that are sampled at the plasma–void interfaces and sent directly into the void regions; and (iii) molecules that are created at the divertor targets. Recycling of ions and fluid atoms incident at the targets as atoms is incorporated in the boundary condition of the fluid model (Eq. (2)). Hence, kinetic source type (iii) only contains the recycling as molecules.

The recycling sources of type (i) are already present in the full kinetic MC simulation. In SOLPS-ITER, bulk ions are sampled from a truncated (drifting) Maxwellian distribution with local ion properties and immediately reflected back into the plasma as an atom or molecule. The reflected atoms and molecules are also treated kinetically in the spatially hybrid approach, identically to the fully kinetic simulation. For source type (ii), the initial particle position is distributed according to the incident fluid atom flux density, given by $-\int_{\mathbf{v}\cdot\boldsymbol{\nu}\leq 0}\boldsymbol{\Gamma}_a(\mathbf{v})\cdot\boldsymbol{\nu}\mathrm{d}\mathbf{v}$, with $\boldsymbol{\Gamma}_a(\mathbf{v})$ defined as a truncated Maxwellian (Eq. (1)). Then, the particle velocity is sampled from the local truncated Maxwellian and sent directly into the void region. Finally, for source type (iii), the source strength follows from the estimated molecular particle flux density Γ_m, given by

$$\Gamma_m = -\int_{\mathbf{v}\cdot\boldsymbol{\nu}\leq 0}(1-R_f(\mathbf{v}))(\boldsymbol{\Gamma}_i(\mathbf{v})+\boldsymbol{\Gamma}_a(\mathbf{v}))\cdot\boldsymbol{\nu}\mathrm{d}\mathbf{v}, \tag{5}$$

with $\boldsymbol{\Gamma}_i(\mathbf{v})$ and $\boldsymbol{\Gamma}_a(\mathbf{v})$ defined by respectively Eqs. (3) and (1). Molecules are emitted into the plasma as thermal particles, i.e., with a Maxwellian energy and cosine angular distribution.

When kinetic atoms hit a solid wall, they are either reflected as fast atoms or thermally released as molecules, with the probability of fast reflection $R_f(\mathbf{v})$ determined by the TRIM database. When an atom from source type (ii) re-enters the plasma region, it is treated kinetically until it ionizes. This way (and additionally due to a kinetic treatment of the recycling sources from type (i)), the spatially hybrid method partially accounts for kinetic effects in the far SOL and PF regions.

2.3. Atomic and molecular interactions

An advantage of the hybrid approach is that the same set of atomic and molecular interactions is used as in a fully kinetic simulation. The cross-section and rate-coefficient expressions are taken from the AMJUEL database [16]. Table 1 gives the set of interactions that we consider in this paper (dealing with a pure deuterium (D) plasma). The fluid atom model contains the first four reactions of Table 1 [12]. This way, the standard reactions for D atoms [17] are incorporated in the fluid description, except for neutral–neutral collisions. The kinetic treatment of the molecules facilitates taking the same set of molecular reactions into account in the hybrid approach as in the fully kinetic simulation. This means that the set of molecular reactions could be easily extended further. The transport of the molecular ions D_2^+ is neglected and it is assumed that D_2^+ immediately reacts at the point of creation.

By comparing the atom charge-exchange mean free path λ_{cx} to a typical macroscopic length scale, one obtains a good indicator for the validity of a fluid approach. Table 2 gives an idea of the charge-exchange mean-free-path length as a function of the ion temperature. The ion density (n_i) needs to be large enough to justify the use of a fluid approach in a certain region. If we for example assume a characteristic length scale of 0.01 m and T_i between 1 and 10 eV, the ion density needs to be much larger than 10^{20} m^{-3} to justify the use of a fluid approach.

We assess two approaches for the treatment of dissociated molecules, i.e., atoms resulting from the dissociation reactions in Table 1: (i) the resulting atoms are treated kinetically and followed in EIRENE; and (ii) the resulting atoms enter the fluid atom model by means of source contributions. Whereas approach (i) is expected to have the largest accuracy, the CPU time reduction might be limited compared to approach (ii), especially for detached cases where molecules can be the dominant contribution in the recycling sources.

Table 1
Overview of considered atomic and molecular interactions, with the corresponding reaction number in the AMJUEL database.

Reaction	Type	AMJUEL
$D^+ + e \rightarrow D$ + photon	Radiative recombination	2.1.8
$D^+ + 2e \rightarrow D + e$	Three-body recombination	2.1.8
$D + e \rightarrow D^+ + 2e$	Ionization	2.1.5
$D + D^+ \rightarrow D^+ + D$	Charge exchange	3.1.8
$D_2 + e \rightarrow D_2^+ + 2e$	Ionization	2.2.9
$D_2 + e \rightarrow 2D + e$	Dissociation	2.2.5 g
$D_2 + D^+ \rightarrow D_2 + D^+$	Elastic	0.3T
$D_2^+ + e \rightarrow 2D^+ + 2e$	Dissociative ionization	2.2.11
$D_2^+ + e \rightarrow 2D$	Dissociation	2.2.14

Table 2
Atom charge-exchange mean free path multiplied by the ion density for typical values of the ion temperature. We assume that the atom has an energy of 3 eV.

T_i [eV]	0.1	1	10	100
$\lambda_{cx} n_i$ [10^{19} m^{-2}]	0.16	0.14	0.079	0.037

3. Setup of the test case

In this paper, we explore the spatially hybrid method for JET ITER-like wall L-mode plasmas from Ref. [18]. Beryllium is used for the main-chamber wall and tungsten for the divertor plasma-facing components. We consider a low-triangularity magnetic equilibrium ($\delta \sim 0.2$) with inner strike point at the vertical plate and outer strike point at the horizontal plate, as shown in Fig. 1.

The plasma current and toroidal magnetic field are 2.5 MA and 2.5 T, respectively. The heating power consists of 1.3 MW Ohmic heating and 1.6 MW neutral-beam power. We assume that 0.7 MW is radiated in the core. The remaining 2.2 MW is equally distributed over the ions and electrons and uniformly spread over the core–edge boundary. We assume an albedo pump coefficient of 0.94 at the pump surfaces that are indicated in Fig. 1. We impose a fixed plasma density n_{core} at the core boundary to obtain a plasma that is relevant for a certain regime. The anomalous plasma diffusion coefficients are radially varying and determined in Ref. [18] to approximate the measured outer midplane profiles of n_e (electron density), T_e, and T_i for a low-recycling case with kinetic neutrals.

To evaluate the improvements of the spatially hybrid approach compared to a purely fluid neutral description, we compare in Section 4 the simulations with kinetic and hybrid neutral models to B2.5 standalone simulations with a purely fluid neutral model. When a purely fluid neutral model is used, the neutral solution is also restricted to the plasma grid. Plasma and neutral recycling is imposed directly at the outermost plasma grid surfaces, instead of at the true vessel boundaries. Hence, $R_f(\mathbf{v}') \not\equiv 0$ in Eq. (2) at a plasma–void interface. We assume complete reflection at the interface in the SOL and an albedo reflection coefficient of 0.94 at the PF boundary to simulate pumping. Explicit treatment of the molecules is avoided by assuming that they dissociate immediately at the surface and are emitted isotropically as (fluid) atoms with an energy of 3 eV, in agreement with the Franck–Condon dissociation process. This way, we obtain a completely deterministic fluid model. As a summary, Table 3 gives an overview of the different neutral models that we compare in the next section.

We use the random noise averaging technique from Ref. [19], for which different outputs of interest are averaged over many iterations to reduce the statistical noise on the results.

Table 3
Overview of the different neutral models, indicating the treatment of the different types of particles.

Model	Atoms from volumetric recombination	Atoms from target surface recombination	Atoms at plasma–void interfaces	Atoms from molecular dissociation	Molecules
Kinetic	Kinetic	Kinetic	Kinetic	Kinetic	Kinetic
Fluid	Fluid	Fluid	Fluid (no voids)	–	3 eV atoms
Hybrid 1	Fluid	Fluid	Kinetic	Kinetic	Kinetic
Hybrid 2	Fluid	Fluid	Kinetic	Fluid	Kinetic

4. Results

4.1. Divertor target plasma profiles

For a low-density case ($n_{\text{core}} = 2.0{\cdot}10^{19}$ m^{-3}), there are large discrepancies between simulations with fully kinetic and purely fluid neutrals due to the relatively large charge-exchange mean free paths in major parts of the domain. Both hybrid approaches (with atoms resulting from molecular dissociation treated as kinetic or fluid) significantly reduce the fluid–kinetic discrepancies for the target plasma profiles (as can be seen in Fig. 2a–b). The target profiles are plotted as a function of the distance from the separatrix along the target plate $s - s_{\text{sep}}$ ($s - s_{\text{sep}} < 0$ for the PF region and $s - s_{\text{sep}} > 0$ for the SOL). As expected, treating the dissociated atoms kinetically is more accurate. For an increased density ($n_{\text{core}} = 4.0 \cdot 10^{19}$ m^{-3}), also the B2.5 standalone simulation with purely fluid neutrals gives accurate results for n_e, especially at the inner target (Fig. 2c–d). Nevertheless, the spatially hybrid approach successfully reduces the fluid–kinetic discrepancies for the electron temperature.

4.2. Neutral density profiles

Although in general the hybrid approaches improve the atomic and molecular density profiles compared to a simulation with purely fluid neutrals, the hybrid-kinetic discrepancies remain larger than for the target plasma profiles in Fig. 2. Fig. 3a–b show the poloidal neutral profiles (n_a and n_m for the atomic and molecular density, respectively) of the pink flux tube in Fig. 1 in the vicinity of the outer target. Especially for the low-density case, we see a large reduction of the fluid–kinetic discrepancy for the atomic density (left hand side of Fig. 3a). For both the low- and high-density cases, the hybrid approaches underestimate the atomic density near the outer target plate. Hence, it seems that the fluid description is not valid near the target. We expect that the fluid models will be more accurate for ITER and DEMO cases with still higher plasma density and macroscopic length scales, which further increase the atom collisionality. The larger neutral density in the vicinity of the target for the simulation with fluid neutrals for $n_{\text{core}} = 4.0 \cdot 10^{19}$ m^{-3}, is due to the additional contribution of 3 eV atoms, which replace the explicit treatment of the molecules.

The hybrid methods give more accurate results for the upstream neutral profiles (Fig. 3c–d). As expected, the accuracy increases with a kinetic treatment of atoms resulting from molecular dissociation. The increased accuracy of the upstream neutral profiles compared to a simulation with purely fluid neutrals proves the success of using the spatially hybrid approach.

The fact that the hybrid-kinetic discrepancy is much smaller for the plasma state than for the atomic density profiles is confirmed by running a single fully kinetic EIRENE iteration on the converged background plasmas obtained by the fluid and hybrid simulations. This way, we get an increased accuracy for the atomic density solutions (see Fig. 4). We conclude that a validation of simulations with hybrid neutrals with diagnostics that involve the atomic density (e.g., deuterium line radiation) requires at least an additional fully kinetic iteration on the converged hybrid plasma solution.

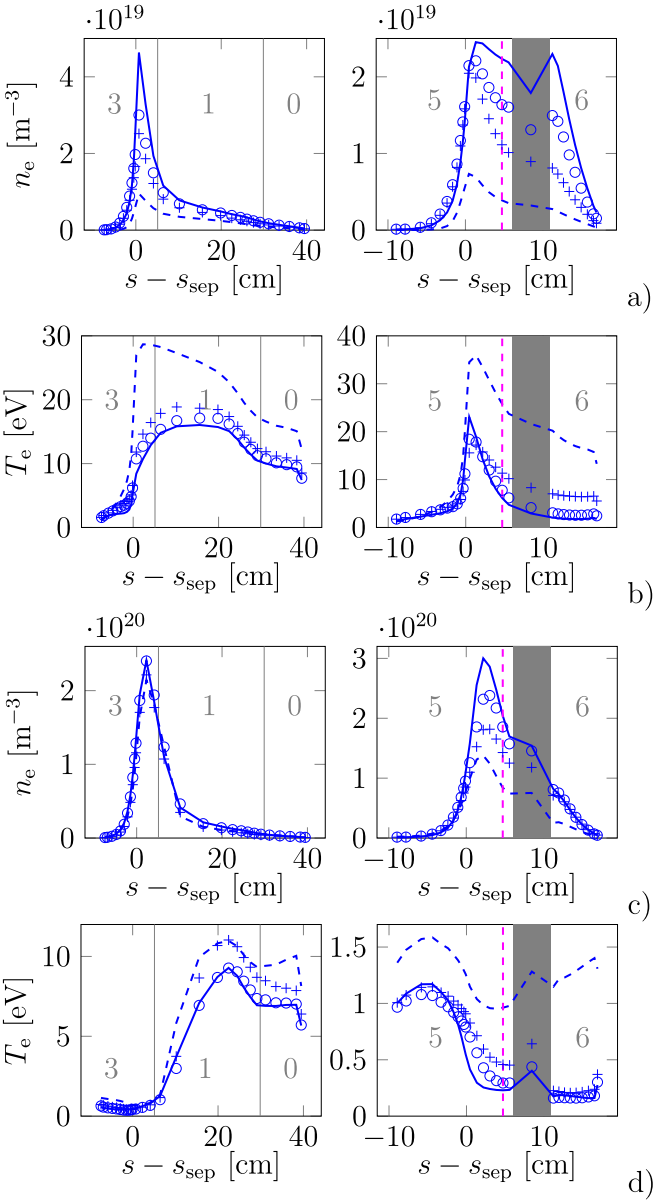

Fig. 2. Divertor target plasma profiles: simulations with fully kinetic neutrals (solid lines), purely fluid neutrals (dashed lines), hybrid neutrals with atoms resulting from molecular dissociation treated kinetically (hybrid 1 in Table 3) (circular marks), and hybrid neutrals with atoms resulting from dissociation treated as fluid (hybrid 2 in Table 3) (pluses). (a)–(b) $n_{\text{core}} = 2.0 \cdot 10^{19}$ m^{-3}; (c)–(d) $n_{\text{core}} = 4.0 \cdot 10^{19}$ m^{-3}. Figures at the left hand side correspond to the inner target and figures at the right hand side to the outer target. The gray lines and numbers indicate the different tile positions (see Fig. 1), with the gray shaded area corresponding to the step between tile 5 and 6. The pink dashed lines in the outer target plots indicate the strike-point location of the flux tube of interest for the neutral profiles in Section 4.2 (see Fig. 1).

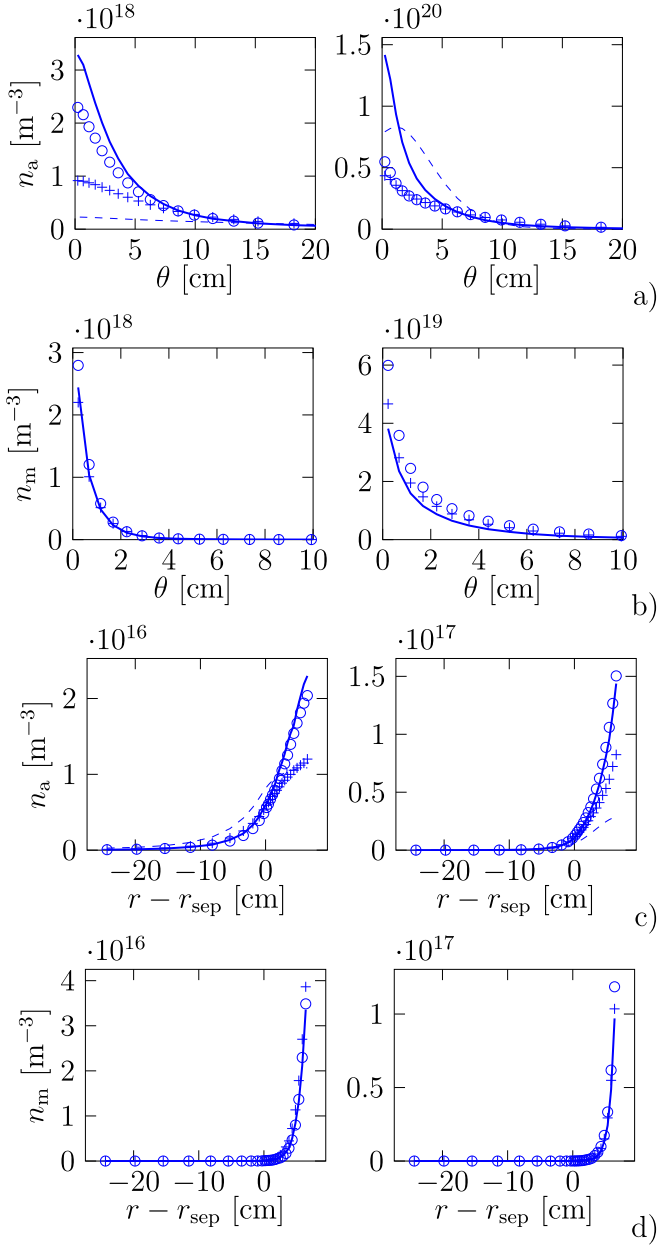

Fig. 3. Neutral density profiles: simulations with fully kinetic neutrals (solid lines), purely fluid neutrals (dashed lines), hybrid neutrals with atoms resulting from molecular dissociation treated kinetically (hybrid 1 in Table 3) (circular marks), and hybrid neutrals with atoms resulting from dissociation treated as fluid (hybrid 2 in Table 3) (pluses). (a)–(b) poloidal profiles in the vicinity of the outer target (see pink dashed line in Fig. 1), as a function of the poloidal distance from the outer target θ; (c)–(d) radial profiles further upstream (yellow dotted line in Fig. 1), as a function of the radial distance from the separatrix $r - r_{sep}$. Left hand side: $n_{core} = 2.0 \cdot 10^{19}$ m^{-3}; right hand side: $n_{core} = 4.0 \cdot 10^{19}$ m^{-3}.

4.3. Quantification of void, molecular, and kinetic effects on the target plasma profiles

The discrepancies between the simulations with fully kinetic and purely fluid neutrals (respectively solid and dashed lines in Fig. 2) can be originating from four possible effects: (i) the absence of void regions in fluid neutral simulations (void effects); (ii) no explicit treatment of molecules in the fluid neutral model; (iii) errors from the fluid limit approximation, i.e., kinetic effects; and (iv) numerical errors.

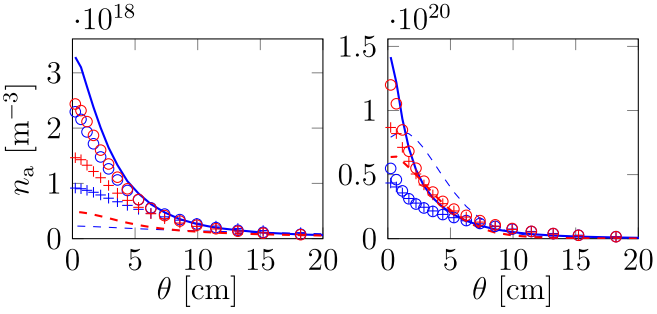

Fig. 4. Poloidal atomic density profiles in the vicinity of the outer target (see pink dashed line in Fig. 1): simulations with fully kinetic neutrals (solid lines), purely fluid neutrals (dashed lines), hybrid neutrals with atoms resulting from molecular dissociation treated kinetically (hybrid 1 in Table 3) (circular marks), and hybrid neutrals with atoms resulting from dissociation treated as fluid (hybrid 2 in Table 3) (pluses). Blue: original solution from Fig. 3; red: single fully kinetic EIRENE iteration on converged background plasma state.

The total numerical error consists of a discretization error, finite-sampling bias, convergence error and statistical error. The sum of the convergence error and finite-sampling bias is typically inversely proportional to the number of MC histories P [19]. When averaging the solution over I iterations, the statistical error scales with $1/\sqrt{PI}$. In our simulations, we make P and I sufficiently large ($P \sim 100\,000$ and $I \sim 10\,000$) to make the influence of the convergence error, finite-sampling bias, and statistical error negligible. Hence, the discretization error is the dominant numerical error contribution in our simulations. Although Ref. [20] shows that the discretization error on the grids typically used for plasma edge simulations could be up to ~50%, we study the performance of the hybrid approach on a typical grid used for many JET simulations [18,21] and leave a grid resolution study for future research.

For this JET case, the kinetic and void effects on the plasma state dominate over the molecular effects. We prove this by gradually excluding the void regions and molecules from the kinetic and hybrid simulations. Fig. 5 shows the results for the outer target profiles. The blue solid and dashed lines correspond to the solutions with respectively fully kinetic and purely fluid neutrals, repeated from Fig. 2.

To quantify the effects of the void regions (i), we exclude the void regions from the simulation with fully kinetic neutrals and apply the same boundary conditions at the artificial walls at the last simulated flux surfaces as in the fluid neutral model (see Section 3), but with still an explicit treatment of the molecules. The PF albedo pump coefficient acts on both the incident atoms and molecules. The solution without void regions (red solid lines in Fig. 5) even deviates more from the fluid solution for $n_{core} = 2.0 \cdot 10^{19}$ m^{-3}, proving that there are other effects that play an important role in causing fluid–kinetic discrepancies.

Subsequently, we assess the molecular effects (ii) by excluding the molecules from the kinetic simulation without void regions (green solid lines). Thermally released particles at the wall are emitted isotropically as atoms with an energy of 3 eV, similar as in the fluid approximation (see Section 3). We conclude that the molecular effects are limited compared to the magnitude of the fluid–kinetic discrepancies. Because of the remaining differences between the blue dashed and red solid lines in Fig. 5, we conclude that the kinetic effects play an important role in causing fluid–kinetic discrepancies. By excluding the void regions from a hybrid simulation with exclusively atoms (green circles), we show that a kinetic treatment of the recycled/reflected neutrals at the PF and outer SOL boundaries already improves the results. This proves the importance of a (partially) kinetic treatment for atoms in some regions of the plasma edge. Similar conclusions are valid for the inner target.

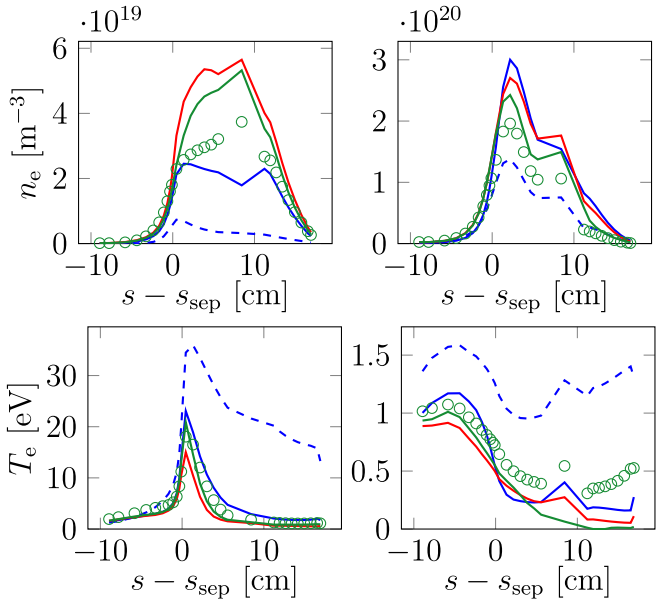

Fig. 5. Outer target plasma profiles from simulations with different neutral models: fully kinetic with void regions and molecules (blue solid lines), purely fluid and hence no void regions and no molecules (blue dashed lines), fully kinetic without void regions with molecules (red solid lines), fully kinetic without void regions and exclusively atoms (green solid lines), and hybrid without voids and exclusively atoms (green circles). Left hand side: $n_{core} = 2.0 \cdot 10^{19}$ m^{-3}; right hand side: $n_{core} = 4.0 \cdot 10^{19}$ m^{-3}.

4.4. Performance assessment

In this section, we compare the statistical errors for a certain CPU time in the averaging phase for the kinetic and hybrid simulations. For each simulation, we use a total amount of 100 000 MC particles for each iteration, distributed over the strata according to their source strengths. Due to the expected $1/\sqrt{I}$ scaling [19], the (relative) statistical error on a certain output of interest ϕ can be written as

$$\epsilon_{s,\phi} = \frac{A_\phi}{\sqrt{I}} \sqrt{\frac{CPU_k}{CPU_{it}}}, \tag{6}$$

with CPU_{it}/CPU_k the CPU time for a single iteration scaled with the CPU time for a single iteration for the simulation with fully kinetic neutrals. CPU_{it}/CPU_k is obviously equal to 1 for the simulations with fully kinetic neutrals. By comparing A_ϕ for different outputs, we observe the statistical error reduction for the same computational time.

We conclude that there is a significant statistical error reduction for both hybrid simulations for the electron density and temperature at the strike-point location, as shown in Table 4 (subscripts 'it' and 'ot' denote the inner and outer target, respectively). As expected, the deterministic treatment of the atoms resulting from molecular dissociation leads to the largest statistical error reduction. Finally, it should be noted that the square of the ratio of A_ϕ from the simulation with kinetic neutrals and A_ϕ from a simulation with hybrid neutrals corresponds to the speed-up in the averaging process of the hybrid approach for the same relative statistical error on ϕ as the simulation with fully kinetic neutrals.

The fact that we use a fixed amount of particles means that there is solely a redistribution over the strata for the different simulations. The reduction of the amount of particles at the targets due to a fluid treatment of recycled atoms is compensated by an increase of particles sampled at the plasma–void interfaces. For the hybrid approach with a kinetic treatment of the atoms from dissociation, we observe that $CPU_{it}/CPU_k \approx 1.46$ for $n_{core} = 2.0 \cdot 10^{19}$ m^{-3} and $CPU_{it}/CPU_k \approx 1$ for $n_{core} = 4.0 \cdot 10^{19}$ m^{-3}. Hence, there is even an increase of the hybrid single-iteration CPU time due to an increased overhead cost from the additional atom background species and additional strata and the redistribution of the fixed number of particles over the different strata. The earlier termination of a particle trajectory by absorbing it in the fluid model after dissociation leads to a reduction of CPU_{it}/CPU_k, i.e., $CPU_{it}/CPU_k \approx 0.83$ for $n_{core} = 2.0 \cdot 10^{19}$ m^{-3} and $CPU_{it}/CPU_k \approx 0.71$ for $n_{core} = 4.0 \cdot 10^{19}$ m^{-3}. We conclude that the reduction of the CPU cost for the transient phase is fairly limited for a fixed amount of particles. Also the large share of molecules to the EIRENE computational cost limits the potential single-iteration CPU-time reduction. Hence, one can benefit from a (partially) deterministic treatment of the molecules.

Table 4
Scaling coefficients A_ϕ for the statistical error [%]: the model names correspond to Table 3.

	$A_{n_{e,it}}$	$A_{n_{e,ot}}$	$A_{T_{e,it}}$	$A_{T_{e,ot}}$
$n_{core} = 2.0 \cdot 10^{19}$ m^{-3}				
Kinetic	4.18	5.23	5.39	5.01
Hybrid 1	2.51	1.56	2.25	1.75
Hybrid 2	1.82	1.18	1.60	1.31
$n_{core} = 4.0 \cdot 10^{19}$ m^{-3}				
Kinetic	1.72	3.07	6.25	9.61
Hybrid 1	1.33	1.45	2.14	1.92
Hybrid 2	1.01	1.07	1.86	1.65

5. Conclusions and outlook

The spatially hybrid fluid–kinetic approach described in this paper is able to significantly reduce the discrepancies between simulations with purely fluid and fully kinetic neutrals, at least for a JET L-mode case. The hybrid approach with a kinetic treatment of the atoms resulting from molecular dissociation (approach 1) reduces the CPU time in the averaging process, compared to simulations with fully kinetic neutrals, with on average a factor 7 for a low-density case and 10 for a high-density case for the same statistical error on the electron strike-point densities and temperatures. When absorbing the atoms resulting from dissociation in the fluid part (approach 2), these speed-up factors further increase to 12 and 14 for the low- and high-density case, respectively, at the expense of accuracy.

For simulations without molecules, we observe a clear reduction of the fluid–kinetic discrepancies when treating the atoms originating at the plasma–void interfaces kinetically. Therefore, we expect that the accuracy of hybrid approach 2 can be increased by treating the atoms resulting from dissociation of the molecules sampled at the plasma–void interfaces kinetically. Hence, a combination of approach 1 and 2 could be the balance between accuracy and computational cost.

As future work, we intend to assess the accuracy and performance of the spatially hybrid approach in the presence of plasma drifts. The assumption of dominant atom flow parallel to the magnetic field might be violated due to charge-exchange collisions with ions that have a large perpendicular drift velocity component. Finally, we plan to eliminate the remaining hybrid-kinetic discrepancies by applying a micro-macro/δf method [9], or a hybrid method based on fluid–kinetic transition sources [22]. Also the use of flux limiters can reduce the fluid–kinetic discrepancies [23].

CRediT authorship contribution statement

N. Horsten: Conceptualization, Methodology, Software, Validation, Formal analysis, Writing - original draft. **M. Groth:** Conceptualization, Writing - review & editing, Supervision, Project administration. **M. Blommaert:** Methodology, Software, Writing - review & editing. **W. Dekeyser:** Methodology, Software, Writing - review & editing. **I. Paradela Pérez:** Data curation. **S. Wiesen:** Data curation.

Table 5
MDSplus shot numbers for different values of n_{core} [m^{-3}]. See Table 3 for an overview of the models.

Model	$2.0 \cdot 10^{19}$	$4.0 \cdot 10^{19}$
Kinetic	182012	182015
Fluid	182010	182011
Hybrid 1	182014	182016
Hybrid 2	182013	182017
Kinetic, no voids	182026	182027
Kinetic, no voids, no molecules	182028	182029
Hybrid, no voids, no molecules	182030	182031

Declaration of competing interest

The authors declare that they have no known competing financial interests or personal relationships that could have appeared to influence the work reported in this paper.

Acknowledgments

This work has been carried out within the framework of the EUROfusion Consortium and has received funding from the Euratom research and training programme 2014–2018 and 2019–2020 under grant agreement No 633053. The views and opinions expressed herein do not necessarily reflect those of the European Commission.

Parts of the work are supported by the Research Foundation Flanders (FWO), Belgium under project grant G078316N.

Appendix. MDSplus shot numbers

The simulations are written to the MDSplus server at IPP Garching. Table 5 gives the different shot numbers.

References

[1] S. Wiesen, D. Reiter, V. Kotov, M. Baelmans, W. Dekeyser, A. Kukushkin, S. Lisgo, R. Pitts, V. Rozhansky, G. Saibene, et al., The new SOLPS-ITER code package, J. Nucl. Mater. 463 (2015) 480–484.
[2] X. Bonnin, W. Dekeyser, R. Pitts, D. Coster, S. Voskoboynikov, S. Wiesen, Presentation of the new SOLPS-ITER code package for tokamak plasma edge modelling, Plasma Fusion Res. 11 (2016) 1403102.
[3] D. Reiter, M. Baelmans, P. Börner, The EIRENE and b2-EIRENE codes, Fusion Sci. Technol. 47 (2) (2005) 172–186.
[4] A. Kukushkin, H. Pacher, V. Kotov, G. Pacher, D. Reiter, Finalizing the ITER divertor design: The key role of SOLPS modeling, Fusion Eng. Des. 86 (12) (2011) 2865–2873.
[5] D. Knoll, P. McHugh, S. Krasheninnikov, D. Sigmar, Simulation of dense recombining divertor plasmas with a Navier–Stokes neutral transport model, Phys. Plasmas 3 (1) (1996) 293–303.
[6] M. Rensink, L. Lodestro, G. Porter, T. Rognlien, D. Coster, A comparison of neutral gas models for divertor plasmas, Contrib. Plasma Phys. 38 (1–2) (1998) 325–330.
[7] M. Furubayashi, K. Hoshino, M. Toma, A. Hatayama, D. Coster, R. Schneider, X. Bonnin, H. Kawashima, N. Asakura, Y. Suzuki, Comparison of kinetic and fluid neutral models for attached and detached state, J. Nucl. Mater. 390 (2009) 295–298.
[8] M. Blommaert, N. Horsten, P. Börner, W. Dekeyser, A spatially hybrid fluid-kinetic neutral model for SOLPS-ITER plasma edge simulations, Nucl. Mater. Energy 19 (2019) 28–33.
[9] N. Horsten, G. Samaey, M. Baelmans, A hybrid fluid-kinetic model for hydrogenic atoms in the plasma edge of tokamaks based on a micro-macro decomposition of the kinetic equation, J. Comput. Phys. 409 (2020) 109308.
[10] S. Braginskii, Transport processes in a plasma, Rev. Plasma Phys. 1 (1965) 205.
[11] V. Rozhansky, E. Kaveeva, P. Molchanov, I. Veselova, S. Voskoboynikov, D. Coster, G. Counsell, A. Kirk, S. Lisgo, M. Team, et al., New b2solps5.2 transport code for H-mode regimes in tokamaks, Nucl. Fusion 49 (2) (2009) 025007.
[12] M. Blommaert, W. Dekeyser, N. Horsten, P. Börner, M. Baelmans, Implementation of a consistent fluid-neutral model in SOLPS-ITER and benchmark with EIRENE, Contrib. Plasma Phys. 58 (6–8) (2018) 718–724.
[13] D. Reiter, The EIRENE code user manual, 2009.
[14] N. Horsten, G. Samaey, M. Baelmans, Development and assessment of 2D fluid neutral models that include atomic databases and a microscopic reflection model, Nucl. Fusion 57 (11) (2017) 116043.
[15] W. Dekeyser, X. Bonnin, S. Lisgo, R. Pitts, B. LaBombard, Implementation of a 9-point stencil in SOLPS-ITER and implications for alcator C-mod divertor plasma simulations, Nucl. Mater. Energy 18 (2019) 125–130.
[16] D. Reiter, The Data File AMJUEL: Additional Atomic and Molecular Data for EIRENE, Tech. Rep., FZ Juelich, 2000.
[17] V. Kotov, D. Reiter, R. Pitts, S. Jachmich, A. Huber, D. Coster, et al., Numerical modelling of high density JET divertor plasma with the SOLPS4.2 (b2-EIRENE) code, Plasma Phys. Control. Fusion 50 (10) (2008) 105012.
[18] M. Groth, S. Brezinsek, P. Belo, M. Beurskens, M. Brix, M. Clever, J. Coenen, C. Corrigan, T. Eich, J. Flanagan, et al., Impact of carbon and tungsten as divertor materials on the scrape-off layer conditions in JET, Nucl. Fusion 53 (9) (2013) 093016.
[19] K. Ghoos, W. Dekeyser, G. Samaey, P. Börner, M. Baelmans, Accuracy and convergence of coupled finite-volume/Monte Carlo codes for plasma edge simulations of nuclear fusion reactors, J. Comput. Phys. 322 (C) (2016) 162–182.
[20] K. Ghoos, P. Börner, W. Dekeyser, A. Kukushkin, M. Baelmans, Grid resolution study for b2-EIRENE simulation of partially detached ITER divertor plasma, Nucl. Fusion 59 (2) (2018) 026001.
[21] V. Solokha, M. Groth, S. Brezinsek, M. Brix, G. Corrigan, C. Guillemaut, D. Harting, S. Jachmich, U. Kruezi, S. Marsen, et al., Isotope effect on the detachment onset density in JET ohmic plasmas, Phys. Scr. 2020 (T171) (2020) 014039.
[22] M. Valentinuzzi, Y. Marandet, H. Bufferand, G. Ciraolo, P. Tamain, Two-phases hybrid model for neutrals, Nucl. Mater. Energy 18 (2019) 41–45.
[23] D. Coster, X. Bonnin, B. Braams, D. Reiter, R. Schneider, et al., Simulation of the edge plasma in tokamaks, Phys. Scr. 2004 (T108) (2004) 7.